INFLUENCE OF THE MINIMUM SWERVING DISTANCE ON THE DEVELOPMENT OF POWERED TWO WHEELER ACTIVE BRAKING

Federico Giovannini
Giovanni Savino
Marco Pierini
University of Florence
Italy
Paper Number 11-0258

ABSTRACT

Among driver assistance systems recently applied to PTWs (ABS, CBS, etc.), the autonomous braking without input from the rider, named *Active Braking (AB),* is one of the most promising safety functions. The potential benefits of the AB are encouraging, although the improper activation of the AB is dangerous for the rider. Therefore the triggering must occur only when the vehicle is in stability conditions and the obstacle is no longer avoidable neither by braking nor by swerving.
In the present paper the last-second swerving maneuver is analyzed to identify the minimum swerving distance (L_{sw}) the rider requires to avoid the collision against an obstacle by turning, as an input for the triggering logic of the AB system. A physical model to define the minimum swerving distance is proposed. To validate the model, an experimental campaign was carried out using a scooter equipped with a prototype AB system and involving 12 test riders. The tests showed the good prediction capability of the L_{sw} algorithm for different riding styles and different scenarios with fixed obstacles.

INTRODUCTION

In the last ten years (2000-2009) the number of road fatalities in Europe significantly decreased. In the same period the number of the fatalities in moped accident generally decreased, although the number of motorcycle and scooter fatalities increased in 8 European countries[1]. The motorized two wheelers require countermeasures and especially motorcycles and scooters.
In the automotive field among the state of the art in terms of non-collaborative safety technology is the AEB (Autonomous Emergency Braking) which started to equip some of the high end passenger cars. A similar system was proved to be applicable to PTWs and the potential benefits were shown [1].

[1] International Traffic Safety Data & Analysis Group "IRTAD Road Safety 2010 – Annual Report".

This autonomous braking system for PTWs was named active braking (AB).
The AEB for passenger cars is triggered when the parameter time to collision (TTC) is lower than 1 s [2, 3], i.e. when the collision is substantially unavoidable. Similarly, the AB was designed to deploy when the collision is physically inevitable thus skipping the risk for a dangerous triggering when the rider's maneuvering can still avoid the crash.
The research on the AB system for PTW focused on the car-following configuration along a straight path. This restriction reduces the applicability of the AB although the basic configuration represents a fundamental step for the system development.
The triggering algorithm compares the obstacle distance with the minimum distance needed to avoid the crash either by purely braking or purely swerving. The potential shorter avoidance distance obtained by a combination of braking and swerving will be theoretically investigated.
The present paper focuses on the validation of the model computing the minimum swerving distance. The model was tested with an experimental campaign involving 12 riders who performed last second avoidance maneuvers of a fixed obstacle at different speed and with different obstacle width.

MINIMUM SWERVING DISTANCE

The swerving maneuver was described by several models assuming time-based algorithms [2] and distance-based algorithms [4, 5, 6].
The model proposed in this paper is distance-based and it is used to compute the L_{sw} distance representing the theoretical limit beyond which the obstacle is no more avoidable by an evasive maneuver. Comparing L_{sw} with the distance between the host vehicle and the leading vehicle it is possible to evaluate the possibility to perform the swerving emergency maneuver and avoid the collision. The collision becomes unavoidable if the distance from the obstacle x_{obj} is lower than the braking distance and there is no trajectory available to elude the collision with the obstacle by an evasive maneuver.
The L_{sw} algorithm provides a simplified kinematics of the maneuver based on a steady turn: the detailed dynamics is replaced by a geometric model. The

L_{sw} model is computed under the following hypotheses:

- the PTW performs a steady turn;
- the velocity of the PTW and the velocity of the leading vehicle are constant;
- the radius of the trajectory is the minimum radius (R_{min}) the PTW can achieve according to the maximum feasible roll angle.
- The model assumes constant $R = R_{min}$ along the whole evasive maneuver.

With these hypotheses the real maneuver should take a longer space than the theoretical maneuver. The real maneuver is composed of two parts:

- the initial transient where the rider applies the countersteering action to enter the turn. The trajectory radius in this part of the maneuver (R_{it}) is higher than the radius of the L_{sw} trajectory, $R_{it} > R_{min}$;
- the unsteady curve after entering the turn. The unsteady effects while maneuvering give the possibility to perform the second part of the evasive curve with a radius R_{uc} lower than the R_{min}, $R_{uc} < R_{min}$.

The L_{sw} model assumes that the aforementioned aspects of a real curve compensate each other and the initial transient effects are higher than the unsteady effects. Accordingly the L_{sw} model represents a theoretical limit: the rider cannot avoid a collision with an obstacle by performing the swerving maneuver at a distance lower than the L_{sw} distance.

The curve description using the swerve model takes into account the maximum roll angle (φ_{max}) the PTW can achieve. This parameter is a function of the adherence between the tire and the road. The model considers the maximum value of the side acceleration $a_{y,max}$ constant along the trajectory. Hence the radius of the path is computed according to Equations (1) and (2),

$$R_{min} = \frac{V_{PTW}^2}{a_{y,max}} \tag{1}$$

$$a_{y,max} = g \cdot \tan(\varphi_{max}) \tag{2}$$

where g is the acceleration of gravity and V_{PTW} the PTW velocity. The PTW and the leading vehicle velocities and the obstacle width are the other variables for the L_{sw} model. The L_{sw} curve is computed by the Equation (3),

$$L_{sw} = \sqrt{2 \cdot R_{min} \cdot (\mathrm{b} + \mathrm{e}) + b^2 - e^2} - \mathrm{k} \cdot V_{PTW} \cdot V_{obj} \cdot \arccos\left(\frac{\mathrm{R_{min}} - \mathrm{e}}{\mathrm{R_{min}} + \mathrm{b}}\right) \tag{3}$$

$$\mathrm{k} = \frac{1}{g \cdot \tan(\varphi_{max})} \tag{4}$$

where b is half the width of the host vehicle, e is the side length of the obstacle according to the driving path (Figure 1). The first part of the Equation (3) describes the swerving distance considering

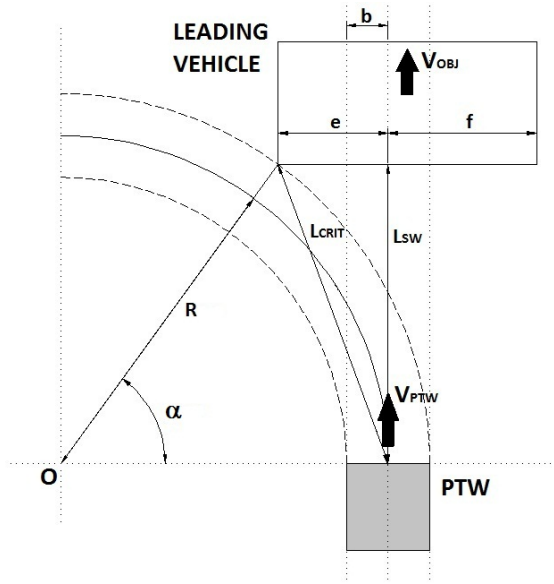

Figure 1. Last-second swerving maneuver.

a static obstacle in front of the host vehicle. The second part takes into account a moving obstacle with velocity V_{obj}. When the vehicle is not aligned with the leading vehicle, a model similar to [7] (Figure 1) can be adopted. It considers the side edge of the obstacle in order to compute whether the evasive maneuver is allowed instead of the L_{sw} distance: the escape trajectory is not available if the leading vehicle has a side edge closer than the distance L_{crit}.

The L_{crit} distance is given by the Equation (5).

$$L_{crit} = \sqrt{{L_{sw}}^2 + e^2} \tag{5}$$

In the present paper the L_{sw} model was adopted.

Comparison with the Kamm's circle

The L_{sw} model is a modified version of the distance-based algorithm using the *Kamm's circle theory* [8] adopted by Kampchen [4] and Schmidt [5]. The Kamm's circle theory considers all the possible trajectories the host vehicle can perform to avoid the collision. It computes the evasive trajectories assuming the maximum side forces that rise in the tire-road interaction. A simplification to the algorithm is to consider the forces between the road surface and the PTW tire as isotropic, hence the ellipse of the adherence coefficient is a circle. The overall acceleration a that a PTW can generate is a combination of the longitudinal acceleration a_x and the side acceleration a_y. The combination of those two components is a function of the angle γ:

$$\begin{cases} a_x = a \cdot \cos(\gamma) \\ a_y = a \cdot \sin(\gamma) \end{cases} \tag{6}$$

The possible evasive maneuvers are functions of the acceleration a, the angle γ and the initial PTW

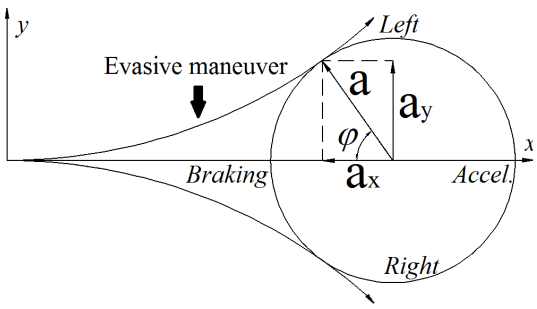

Figure 2. Evasive maneuver computed by the Kamm's circle.

velocity V_{PTW} and they are tangent to a circular region with radius $a_{y,max}$ (Figure 2).
According to the Kamm's circle theory the minimum swerving distance ($L_{sw,K}$) is computed as in Equation (7):

$$L_{sw,K} = \sqrt{\frac{2 \cdot e}{\mu \cdot g \cdot \sin(\gamma)}} \cdot \left(V_{PTW} - V_{obj}\right) + e \cdot \frac{\cos(\gamma) - \frac{d_{obj}}{\mu \cdot g}}{\sin(\gamma)}; \quad (7)$$

$$\gamma: \quad \frac{\left(V_{PTW} - V_{obj}\right) \cdot \cos(\gamma)}{\sqrt{2 \cdot \mu \cdot g \cdot e}} + \frac{1 - \frac{d_{obj}}{\mu \cdot g} \cdot \cos(\gamma)}{\sqrt{\sin(\gamma)}} = 0; \quad (8)$$

where μ is the adherence coefficient and d_{obj} is the deceleration of the leading vehicle. The authors implemented the MAGIC FORMULA by Pacejka [9] for motorcycle tires to compute the adherence coefficient in detail. Hence the main parameters affecting μ without considering the inertial features of the PTW are the sideslip angle and the roll angle. The sideslip angle was set to 1°. To show the differences between the L_{sw} model and the Kamm's circle model the minimum swerving distances are computed in the following conditions:
a. same maximum roll angle;
b. same adherence coefficient.

Case a.

Taking into account different roll angles the models give different minimum swerving distances. As Figures 3a, 3b and 3c show at low values of the roll angle the L_{sw} distance is higher than the distance of the Kamm's model, whereas at high roll angles the situation is inverted.
When comparing the minimum swerving distance using the same maximum roll angle, the two models produce different results. When the roll angle is higher than 30° the L_{sw} distance is lower than the Kamm's swerving distance, therefore the L_{sw} is precautionary. When the roll angle is lower than 30° the Kamm's swerving distance is lower than the L_{sw} distance. Nevertheless those distances are greater than the distances computed with higher roll angles.

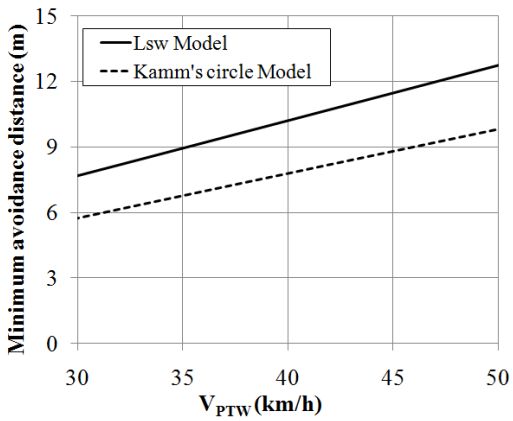

Figure 3a. Comparison between the L_{sw} curve and the Kamm's circle curve considering a roll angle φ_{max} = 15°.

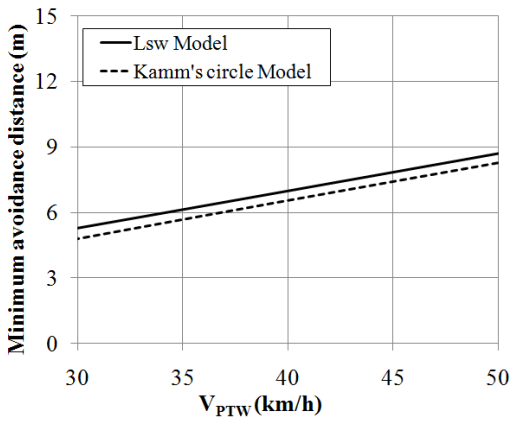

Figure 3b. Comparison between the L_{sw} curve and the Kamm's circle curve considering a roll angle φ_{max} = 30°.

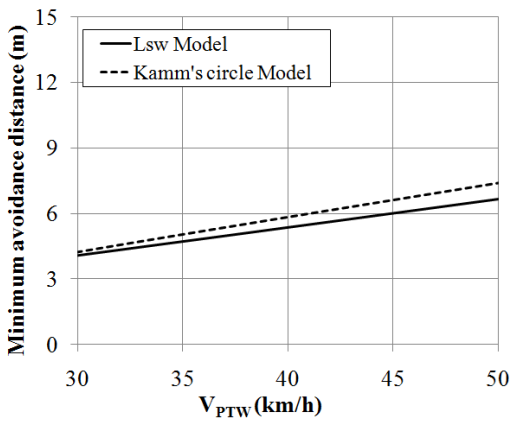

Figure 3c. Comparison between the L_{sw} curve and the Kamm's circle curve considering a roll angle φ_{max} = 45°.

Case b.

When the adherence coefficient is the same the curves are almost overlapped even with different roll angles (Figures 4a, 4b and 4c).

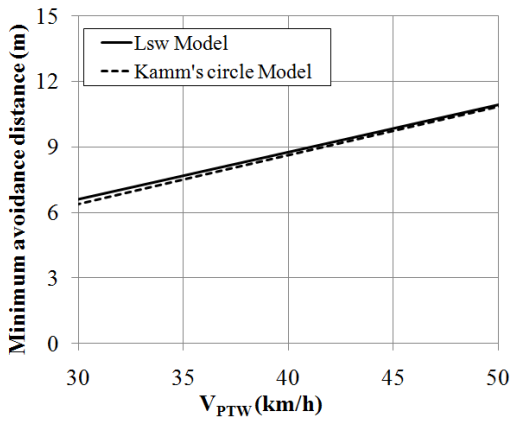

Figure 4a. Comparison between the L_{sw} curve and the Kamm's circle curve considering an adherence coefficient μ = 0.36.

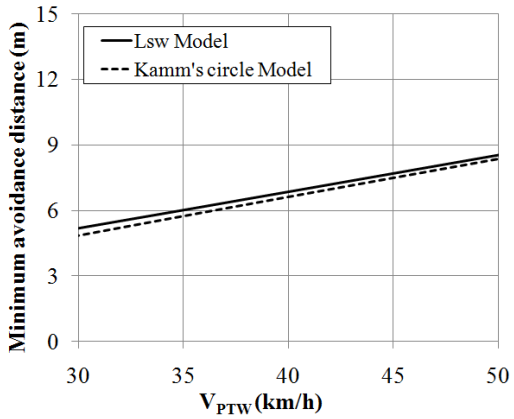

Figure 4b. Comparison between the L_{sw} curve and the Kamm's circle curve considering an adherence coefficient μ = 0.6.

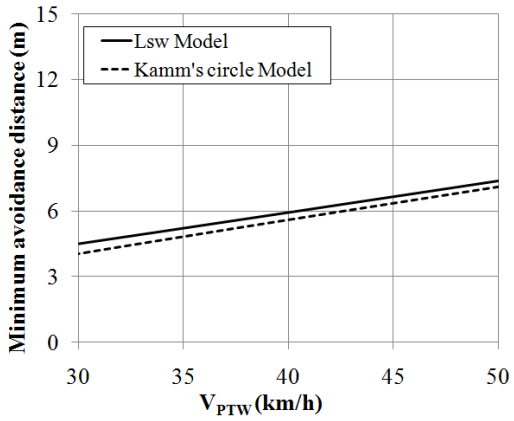

Figure 4c. Comparison between the L_{sw} curve and the Kamm's circle curve considering an adherence coefficient μ = 0.8.

Even if gaps of few centimeters are detected at low velocities between the displayed curves, the minimum swerving distances are the same at different velocities. This aspect is highlighted at low values

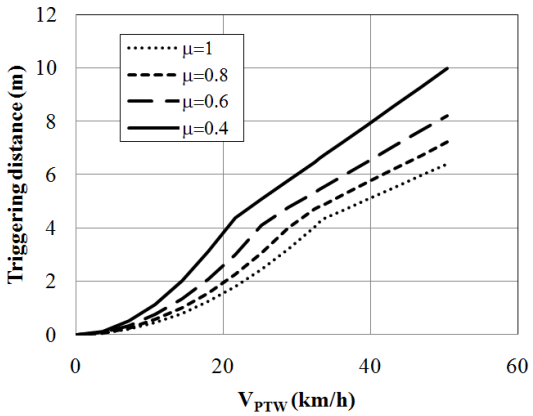

Figure 5. Minimum avoidance distance as a function of the PTW velocity (V_{obj}=0).

of μ where the models overlap over the velocity range.

Potential benefits

The potential benefits of the AB were calculated based on the basic braking model and the L_{sw} method considering the hypothesis of high adherence coefficient: μ=1. When the adherence is low, e.g. in the case of wet surface, the minimum avoidance distance is higher (Figure 5).
As a consequence the collision becomes unavoidable at higher distance and the triggering could occur earlier, thus increasing the potential effectiveness of the AB. However the measurement of μ is still challenging. The approach consisting in taking μ=1 when the actual adherence is lower than 1 does not allow the full exploitation of the AB in all the conditions, although it is precautionary for those cases where the adherence is high. The comparison between L_b and L_{sw} shows that the swerving maneuver is more effective than braking at high velocity (Figure 6). The L_{sw} distance depends on the velocities and it is affected by the maximum achievable roll angle and the obstacle width (Figure 7).
When the maximum roll angle is higher, the minimum swerving distance is lower whereas the wider obstacle produces an increment in the swerving distance. The maximum roll angle in case of fair adherence it is up to 45° but it can be limited for a specific PTW by the actual lateral shape. The obstacle width in a car following configuration can vary from 0.6 m representing a single track vehicle up to 3 m representing a heavy load truck. Focusing on the urban scenario where the speed limit is 50 km/h the swerving maneuver is relevant in the range between 30 km/h and 50 km/h. Therefore the validation of the swerve model was conducted in that speed range.
The benefits are calculated as the reduction of kinetic energy at the impact produced by the AB system compared with the case where the rider does not react. The AB deceleration takes place at the instant when the actual distance is equal to the

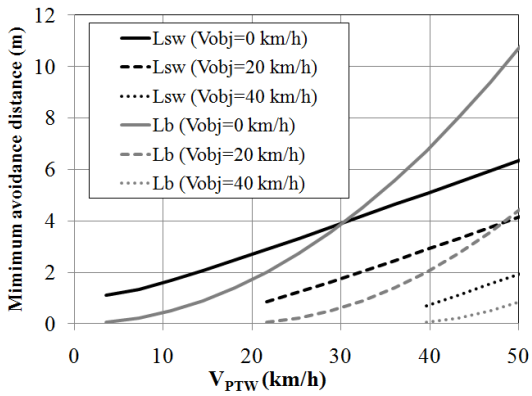

Figure 6. Comparison between the L_{sw} model and the Braking model. Required PTW deceleration d_{req}= 9 m/s^2.

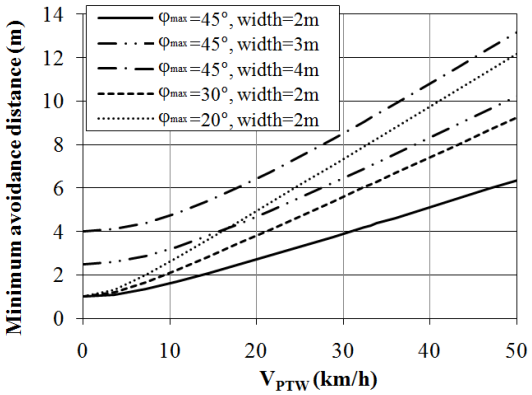

Figure 7. The L_{sw} model taking into account different values of μ and different values of obstacle width.

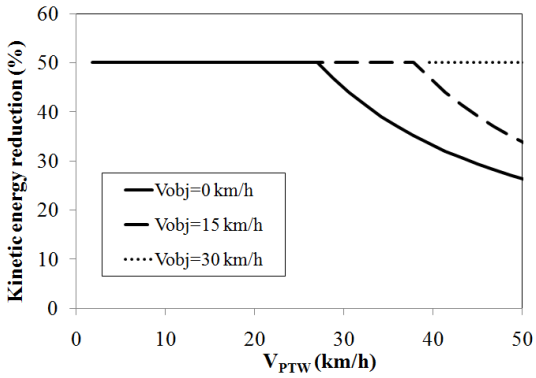

Figure 8. Energy reduction in a collision with different V_{obj}. Required PTW deceleration d_{req}= 8 m/s^2, AB deceleration d_{AB}= 4 m/s^2.

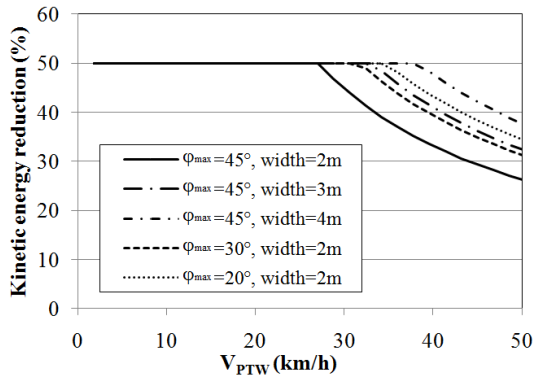

Figure 9. Energy reduction in a collision with different φ_{max} and different obstacle widths. Required PTW deceleration d_{req}= 8 m/s^2, AB deceleration d_{AB}= 4 m/s^2.

theoretical avoidance distance. The system will take care of producing a warning signal to alert the rider 0.3 s in advance to the active deceleration. Moreover the hydraulic system should be pre-loaded in order to obtain the active deceleration without any delay.

Calculation of the theoretical energy reduction was made fixing the AB intervention parameters and varying the obstacle width, the max roll angle and the leading vehicle velocity (Figure 8 and 9).

As shown in the pictures the benefits are influenced by the following parameters:

- obstacle width
- leading vehicle and host vehicle velocity
- φ_{max}.

The value of φ_{max} (the max roll angle during the swerving maneuver) affects the potential benefits of the AB. In particular, the benefits are lower for agile vehicles allowing for higher roll angles. The impact energy reduction is influenced by the obstacle width and is significantly higher when the obstacle is wider. For very narrow obstacles the option to inhibit the AB activation has to be taken into consideration since the benefits are minor and the risk for a false triggering is higher. The benefits are calculated considering the PTW aligned with the tail center of the leading vehicle. When the PTW is not centrally aligned the swerve model in Figure 1 can be adopted. The host PTW velocity influences the potential benefits as well.

Swerve detection

A criterion to identify the distance at which the rider begins the evasive maneuver was defined. The detection the maneuver has started is based on the tilt status of the PTW, considering two parameters:

- the roll angle;
- the roll rate.

The authors defined the beginning of the swerving maneuver at the instant t_d when the PTW reached 5° of roll angle or 25°/s of roll rate. Those values were fixed according to a preliminary analysis on the experimental outcomes. The algorithm based on the roll angle detection gives the possibility to identify the swerving maneuver while performing curves that demand high roll angle and the use of the control of the roll rate in addiction enables the detection of maneuvers characterized by low roll

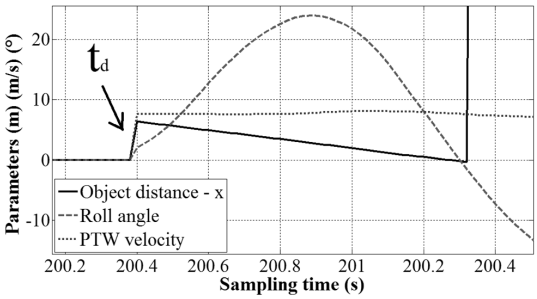

Figure 10. Detection of td instant at the beginning of an evasive maneuver.

angles and quick movements. The Figure 10 shows the detection instant t_d during the emergency evasive maneuver.
The algorithm proposed for the data post processing was used in real time on the control logic system as well. This gave the AB system a tool to identify the beginning of the swerving maneuver and detect the unstable conditions of the PTW, when a AB triggering would be dangerous in theory.

TESTING

An experimental campaign was conducted to compare the theoretical L_{sw} with the swerving spaces of a set of 12 subjects while performing last second swerving maneuvers. The subjects were volunteers with more than 5 years of riding license and different riding experience. The equipment consisted in a 500 cm^3 scooter with high inertia and high wheelbase equipped with sensors including an inertial measurement unit (IMU) and a compact laser scanner located in the front shield (Figure 11). The IMU measured the state parameters of the PTW, whereas the laser scanner measured the distance of the obstacle with fair accuracy. The obstacle distance was also measured with the on board sensor to show a potential solution for the implementation of the AB system. An on board control unit processed the signals and performed the data acquisition.
The tests were performed in empty and free space using a modular obstacle constituted by cardboard boxes (Figure 12). The test trials aimed to investigate the swerving maneuver at different velocities up to 50 km/h and different obstacle widths, the obstacle being static. Before starting the tests, every test rider was given a free amount of time to train with the vehicle and with the avoidance maneuver. The mean settling time was 8 minutes, ranging from 5 to 10. The test run consisted in approaching an obstacle at a target velocity and along a straight trajectory aligned with the centre of the obstacle and performing a last second avoidance maneuver without braking while swerving.
The vehicle started from stationary condition and the obstacle was positioned 60 m far from the PTW.

Figure 11. The scooter and the acquisition system used for the experimental tests.

Figure 12. One of the evasive maneuvers performed in the experimental tests.

Each rider performed several runs at different target velocities and swerved around an obstacle.
The tests were performed with 1.2 m, 1.8 m and 3 m obstacle widths, as summarized in Table 1. The accuracy of the detection of the obstacle position and actual heading/trajectory of the host PTW was not enough to deal with smaller obstacles.

Table 1.
Number of runs performed for each PTW velocity and for each obstacle width.

	30 km/h	40 km/h	50 km/h
1.2 m	4 (left) 4 (right)	4 (left) 4 (right)	4 (left) 4 (right)
1.8 m	-	6	-
3.0 m	-	6	-

A total of 450 tests were performed and 402 of them were considered eligible for the analysis.

Analysis of the swerving maneuvers

The analysis of the data acquired during the tests highlighted different styles among the riders in the first part of the swerving maneuver. The differences regarded the steering angles and the maximum roll

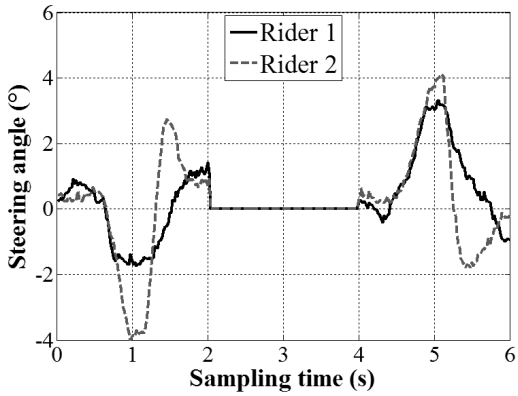

Figure 13a. Comparison of the steering angles between two riders during a right and left side evasive maneuver.

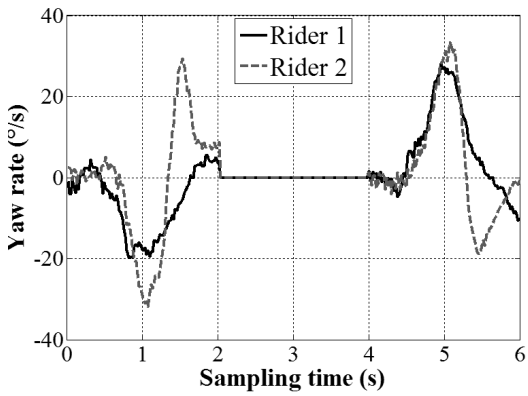

Figure 13b. Comparison of the yaw rates between two riders during a right and left side evasive maneuver.

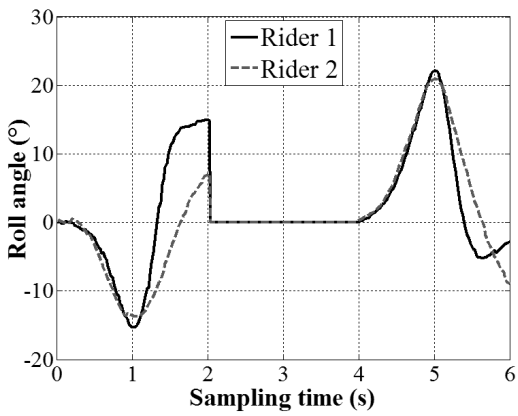

Figure 13c. Comparison of the roll angles between two riders during a right and left side evasive maneuver.

angles achieved while turning. A number of riders applied significantly higher steering rates and large steering angles at the beginning of the maneuver thus obtaining higher yaw rates. This behavior gave the rider the possibility to reduce the radius of the curve trajectory thus reducing the emergency swerving distance. On the contrary other riders applied smaller steering angles associated to higher values of the maximum roll angle. Those riders were compelled to begin the maneuver few meters in advance that the riders that used to apply higher steering angles while turning. Figures 13a, 13b and 13c show the comparison between two riders belonging to the aforementioned classes of driving styles.

Results

For each one of the 402 analyzed runs, the time instant t_d representing the beginning of the swerving maneuver was identified using the swerve detection algorithm in off-line mode.
The quantities V_{PTW} and x_{obj} at time t_d were extracted from the logged data in order to compare the actual swerving space with the theoretical L_{sw} (Figure 14).The index of gap between L_{sw} and x_{obj} was defined as follows:

$$I_g = \frac{x_{obj,t_d} - L_{sw}}{L_{sw}} \qquad (9)$$

In Figures 15a, 15b and 15c the results of the tests are plotted in diagrams showing the value of the gap index for each run as a function of the initial PTW velocity. Each diagram groups the runs performed with a certain obstacle width.
Firstly the whole set of test runs reported a positive outcome in terms of predicted minimum swerving distance. In fact the swerving space utilized by each rider in each test configuration was higher than the theoretical L_{sw} for the specific configuration.
Secondly, the model is able to identify the minimum swerving distance with a limited gap between the theoretical value and the *best cases* of the test runs, both for different PTW velocities and for different obstacle widths. A small gap means that the inhibition of the AB due to the possibility to avoid the collision by swerving is removed at a distance just above the best performance in a real maneuver. This means the benefits of the AB are maximized. When the gap is close to zero it also means that the risk of a false triggering case becomes high, since a very skilled rider might overcome the performances of the test riders thus producing a fault of the L_{sw} model. A negative gap denotes that the swerving maneuver was performed in a distance smaller than the theoretical limit. The runs resulted in no negative gap cases. The L_{sw} model was designed for the car following scenario with a moving lead vehicle and the validation should consider the moving obstacle case. Such a validation campaign is dangerous for the rider since a collision with a light trail is sufficient to cause a fall. Albeit the tests described in the present work were conducted with fixed obstacles the results can be extended to the moving vehicle case with the

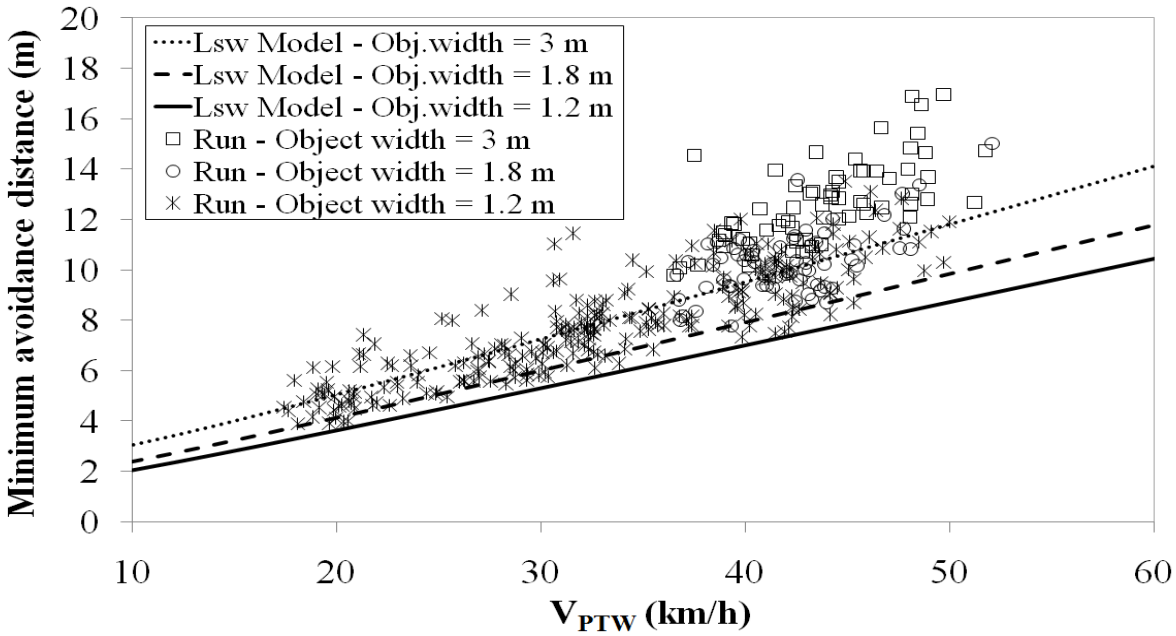

Figure 14. Experimental trials compared with the L_{sw} curves.

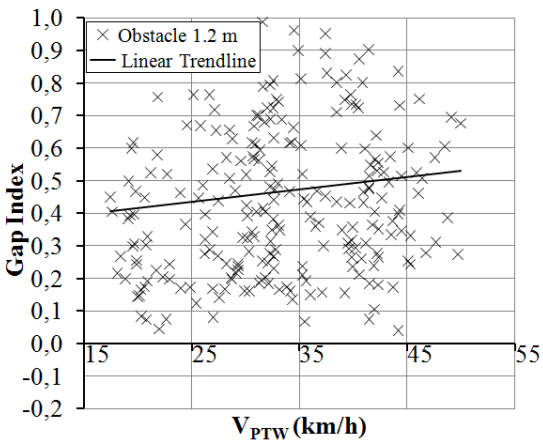

Figure 15a. Gap Index for each run of the experimental test with an obstacle width of 1.2 m

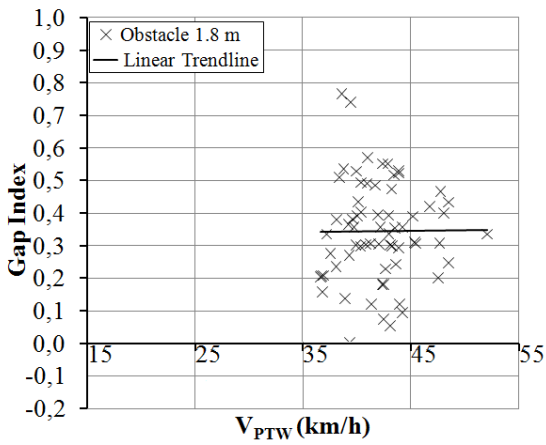

Figure 15b. Gap Index for each run of the experimental test with an obstacle width of 1.8 m

hypothesis that every rider produces the best performances in safer conditions (i.e. with the fixed obstacle). When performing the car following task the swerving spaces are expected to have higher dispersion, always being above the theoretical value L_{sw}. Further research should implement experimental tests dedicated to the validation of the L_{sw} model with a moving obstacle.

CONCLUSIONS

The research for the implementation of the AB is far from the spread in the series vehicles, although the feasibility of the system was proved and the potential benefits are of relevance. Even when the application of the AB is restricted to the basic car following scenario, it is fundamental to prove that the system is reliable and it will not trigger unless

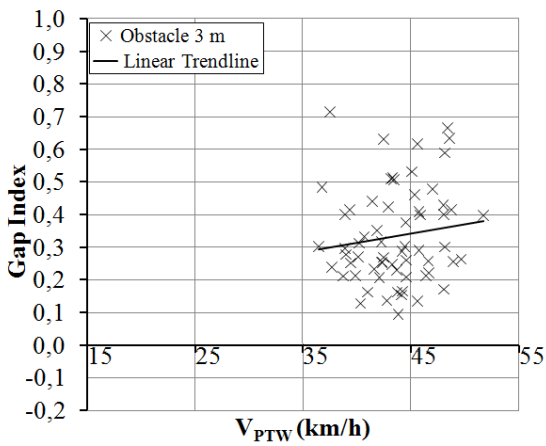

Figure 15c. Gap Index for each run of the experimental test with an obstacle width of 3 m

the PTW is upright and the rider cannot avoid the crash. The feasibility of a last second swerving maneuver is one of the criteria to allow or inhibit the activation of the AB. This work presented an experimental campaign whose results support the validation of the L_{sw} method which estimates the minimum swerving distance with a low computational effort and small margins. The tests showed a good accordance between the theoretical minimum swerving distance and the experimental results conducted with a large scooter. The L_{sw} algorithm is expected to be effective for different kind of PTWs although further investigation is required for a validation on smaller and more agile vehicles.

ACKNOWLEDGMENTS

This research activity conducted by the Centre for Innovation and Safety of Powered Two Wheelers was partially funded by the Province of Prato within the project *Road Safety of Powered Two Wheelers*.

REFERENCES

[1] G. Savino, M. Pierini, R. Grant, R. Frampton, et al. 2010, "PISa Powered two-wheeler Integrated Safety. Development, implementation and testing of PTW integrated safety systems", Proceedings of the 8th International Motorcycle Conference, Cologne, Germany, 4/5 October 2010.

[2] E. Coelingh, A. Eidehall, M. Bengtsson 2010 "Collision Warning with Full Auto Brake and Pedestrian Detection - a practical example of Automatic Emergency Braking", 13th International IEEE Conference on Intelligent Transportation Systems, IEEE, 2010, pp. 155–160.

[3] R. Labayrade, C. Royere, and D. Aubert, "Experimental Assessment of the RESCUE Collision-Mitigation System," IEEE Transactions on Vehicular Technology, vol. 56, January 2007, pp. 89-102.

[4] N. Kampchen, B. Schiele 2009, "Situation assessment of an autonomous emergency brake for arbitrary vehicle-to-vehicle collision scenarios", IEEE Transactions on Intelligent Transportation Systems, vol. 10, pp. 678–687.

[5] C. Schmidt, F. Oechsle, W. Branz 2006, "Research on trajectory planning in emergency situations with multiple objects", IEEE Intelligent Transportation Systems Conference, 2006, pp. 988–992.

[6] G. Savino, A. Penumaka, M. Pierini, N. Baldanzini, B. Roessler 2009, "Design Of The Decision Logic For A PTW Integrated Safety System", Proceedings of the 21st ESV Conference, Stuttgart, Germany, 2009.

[7] M. Dittmer, "Automatic Emergency Braking", IBEO Automobile Sensor GmbH.

[8] B. Breuer, K. H. Bill 2006, "Bremsenhandbuch. Grundlagen, Komponenten, Systeme", Fahrdynamik, Vieweg-Teubner, 2006.

[9] H. B. Pacejka 2006, "Tyre and vehicle dynamics", Butterworth-Heinemann Ltd, 2006.